Impact of tissue photon attenuation in small animal cardiac PET imaging

Nobuyuki Hayakawa [a,b], Tomohiko Yamane [a,b], Anahi-Paula Arias-Loza [b,c], Tetsuya Shinaji [a,b], Hiroshi Wakabayashi [a,b], Constantin Lapa [a], Rudolf A. Werner [a,b], Mehrbod S. Javadi [d], Theo Pelzer [c], Takahiro Higuchi [a,b,*]

[a] Department of Nuclear Medicine, University Hospital Würzburg, Würzburg, Germany
[b] Comprehensive Heart Failure Center, University Hospital Würzburg, Würzburg, Germany
[c] Department of Internal Medicine I, University Hospital Würzburg, Würzburg, Germany
[d] Division of Nuclear Medicine, Russell H. Morgan Department of Radiology, Johns Hopkins University, Baltimore, MD, United States

1. Introduction

In clinical practice, molecular PET imaging using radionuclide tracers provides unique information and is a well-established non-invasive technology in patients with cardiac diseases [1–6]. Recent introduction of non-invasive small animal imaging utilizing high-resolution dedicated small animal positron emission tomography (PET) systems enables longitudinal functional assessment of molecular and cellular cardiovascular events in rodent disease models [7–9]. Since the same platform of PET is well established and routinely used in clinical practice in the human setting, small animal imaging technology is widely expected to play a central role in the context of translation from basic science to clinical medicine [9,10]. However, precise knowledge of the similarities and differences between the small animal and human imaging technologies are of utmost importance, particularly when comparing the results of each modality.

The impact of tissue photon attenuation on quantitative analysis and regional tracer distribution in small animal cardiac PET imaging remains controversial. Due to physical interactions including both absorption and scattering of the primary photons that occur during the travel of the photons through the body, the number of photons detected by PET detectors is reduced. The magnitude of attenuation on a line connecting the two detectors along which the positron emission occurred can be expressed by an exponential attenuation factor $e^{-\mu D}$, where μ is the linear attenuation coefficient and D is the total thickness of the matter [11]. As a result, PET signals originating in the center of homogeneous attenuation materials are underestimated whereas those from the surface are less affected [12]. Furthermore, the heart is surrounded by tissues of varying density such as lung, blood and liver resulting in attenuation variability among ventricular segments in humans (Fig. 1) [13]. Therefore, appropriate attenuation correction (AC) is essential for quantification and routinely applied in clinical PET studies [11,14–16]. In contrast, AC is only occasionally performed in

* Corresponding author at: Comprehensive Heart Failure Center/Department of Nuclear Medicine, University of Würzburg, Oberdürrbacher Strasse 6, 97080 Würzburg, Germany.
E-mail address: thiguchi@me.com (T. Higuchi).

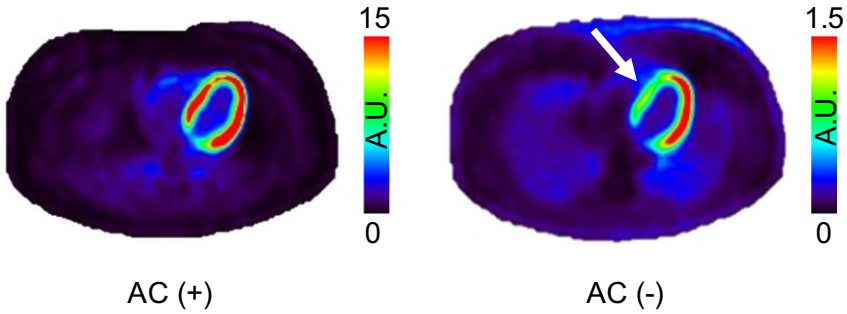

Fig. 1. Example transaxial images of human ^{18}F-FDG PET at the mid-ventricular level with and without attenuation correction (AC). False-positive uptake defect is seen in the septal wall without attenuation correction (white arrow).

small animal cardiac PET studies. The impact of attenuation in small animal imaging is considered to be marginal because of small body size.

The aim of this study is to determine the impact of tissue attenuation on quantitative small animal cardiac PET assessment of global and regional tracer distribution analysis comparing lean and obese rats.

2. Materials and methods

2.1. Animals

Eight male obese Zucker diabetic fatty rats (fa/fa) (obese ZDF rats), a genetic model of obesity and diabetes mellitus [17] (body weight; 370 ± 52 g) and six male Zucker lean rats (ZL lean rats) (body weight; 290 ± 15 g, $p < 0.005$ vs. obese) were used at age of 13 weeks. Experimental protocols were approved by the regional governmental commission of animal protection and were in compliance with the *Guide for the Care and Use of Laboratory Animal* [18].

2.2. PET image acquisition and reconstruction

PET images were acquired using a dedicated small-animal PET scanner (Inveon, Siemens), which provides 12.7 cm axial and 10.0 cm transaxial fields of view and an isotropic reconstructed image resolution of approximately 1.4 mm in full width at half maximum (FWHM). 13 min transmission scans with ^{57}Co (160 MBq) rotating point sources were performed using singles measurement with a narrow energy window of 120–125 keV. Subsequently, under hyperinsulinemic-euglycemic clamp to enhance cardiac activity, approximately 37 MBq of ^{18}F-FDG were administered via the tail vein. A 20 min emission PET acquisition was started 15 min after tracer administration. The acquired data were reconstructed by 2-dimensional ordered subset expectation maximization (OSEM) with 4 iterations and 16 subsets with and without AC. Scatter correction was not conducted.

2.3. Data analysis and statistics

The reconstructed PET images were analyzed using an image processing application, AMIDE (version 1.0.4). To estimate the counts within the left ventricle, 3-dimensional elliptical cylinder regions of interest (ROIs) with 3-mm thickness were manually drawn in whole-body transaxial images both with and without AC to cover the left ventricle at the mid-level. The mean counts in each ROI was measured, and activity reduction by attenuation (%) was calculated as follows,

$$\text{Activity reduction by attenuation } (\%) = (C_{AC} - C_{NAC})/C_{AC} \times 100.$$

Here C_{AC} indicates counts with AC, and C_{NAC} indicates counts without AC.

The chest diameter was defined as the mean of transverse and anteroposterior diameters of the chest at the same level as the heart ROI. Transverse and anteroposterior diameters were measured in the transmission images.

In order to evaluate regional tracer distribution, cylinder ROIs with 3-mm thickness were manually drawn within the anterior, lateral, posterior, and septal walls of left ventricle at the mid-level on the cardiac short axis slices. The mean count in each ROI was measured, and activity reduction by attenuation was calculated for each wall.

Data were expressed with mean ± standard deviation. $P < 0.05$ was considered statistically significant. Chest diameter and activity reduction by attenuation were compared between obese and lean rats using Student's *t*-test. In order to assess regional variation of attenuation, activity reduction by attenuation was assessed among the four myocardial walls using one-way analysis of variance in lean and obese rats.

3. Results

3.1. Impact of tissue attenuation for global cardiac activity

Cardiac activity of both obese ZDF rats and ZL lean rats increased after attenuation correction (Fig. 2). Measured chest diameters were significantly longer in obese ZDF rats (5.6 ± 0.3 cm) than in ZL lean rats (4.5 ± 0.2 cm, $p < 0.0001$). Cardiac activity reduction by attenuation was significantly higher in obese ZDF rats (44.1 ± 2.5%) than in ZL lean rats (35.1 ± 3.1%, $p < 0.0001$).

3.2. Distribution of attenuation among the myocardial walls

The myocardial activity reduction by attenuation in lean and obese rats is shown for each ventricular wall in bar graphs (Fig. 3). No significant differences were found among the left ventricular walls in both ZL lean rats ($p = 0.73$) and obese ZDF rats ($p = 0.65$).

4. Discussion

In this study, we estimated the impact of photon tissue attenuation on small-animal cardiac PET imaging comparing obese and lean rats. Tissue attenuation caused approximately 10% underestimation error in obese rats as compared to lean rats of the same age and could subsequently promote misleading results interpretations of results. Our present findings emphasize the importance of attenuation correction even in small animal PET imaging, especially when performing quantitative comparison of global cardiac tracer accumulation in rats with different body sizes, and/or a longitudinal evaluation with a high likelihood of changes in animal body weight are performed.

The activity of the transmission source [19] and a proper algorithm for AC [20] are crucial in this experiment. In here the use of physical cylinder phantoms with different sizes, permit us to confirmed accuracy of our attenuation correction before animal experiments (Supplemental Fig. 1).

Compared with human studies [21,22], photon tissue attenuation in small rodent PET imaging is considered minor. In a cylinder phantom model with variable diameters, in which a point source is placed at the center, the relation between attenuation and the cylinder diameter is expressed as the following equation: activity reduction by attenuation $= 100\ (1 - e^{-\mu d})$ [11], where d is the diameter of the cylinder object (cm), and coefficient μ is that of acrylic ($= 0.110\ \text{cm}^{-1}$). Our results of tissue attenuation of the heart (activity reduction vs. chest diameter) in mouse, rat and human hearts (unpublished data) are well-matched to the line of the theoretical attenuation of the acrylic phantom (Fig. 4). Although the impact of attenuation in human cardiac PET imaging is as high as 90%, attenuation in small animals such as rat and mouse can also reach up to 20–50% and therefore it should not be ignored when considering absolute quantification in experiments.

There were no significant differences in the regional attenuation distribution pattern between the myocardial walls in both obese and lean

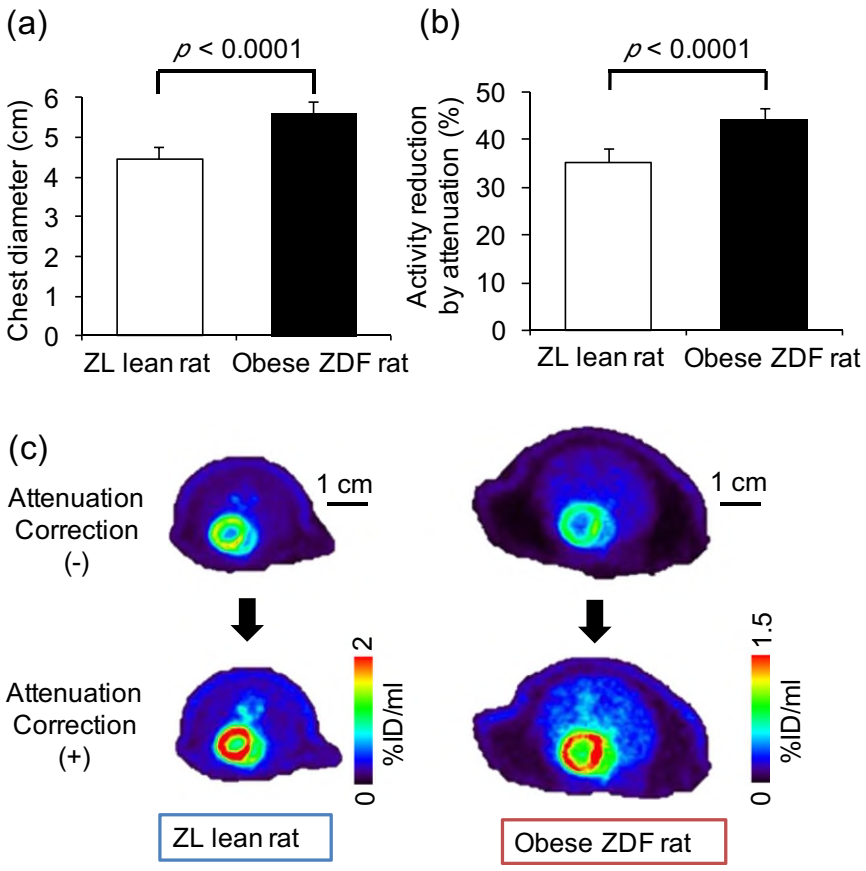

Fig. 2. Bar graphs of chest diameter (a) and cardiac activity reduction by tissue attenuation (b) in Zucker lean (ZL lean rat) and Zucker diabetic fatty rats (obese ZDF rat). Representative transaxial images of a ZL lean rat and an obese ZDF rat with and without attenuation correction (c). The tracer activity of the heart is reduced by tissue attenuation in both groups, but with significantly higher impact in the obese ZDF rats.

rats. In human hearts, it is well recognized that there is a large variation among the walls that can lead to false-positive tracer uptake defects, especially in septal walls if appropriate attenuation correction is not performed (Fig. 1) [21,22]. In contrast, our current results of regional analysis in rat hearts demonstrate only minimal variations and suggest the feasibility to monitor the regional tracer uptake distribution pattern, such as defect sizes in rat models of myocardial infarction, without the need for attenuation correction.

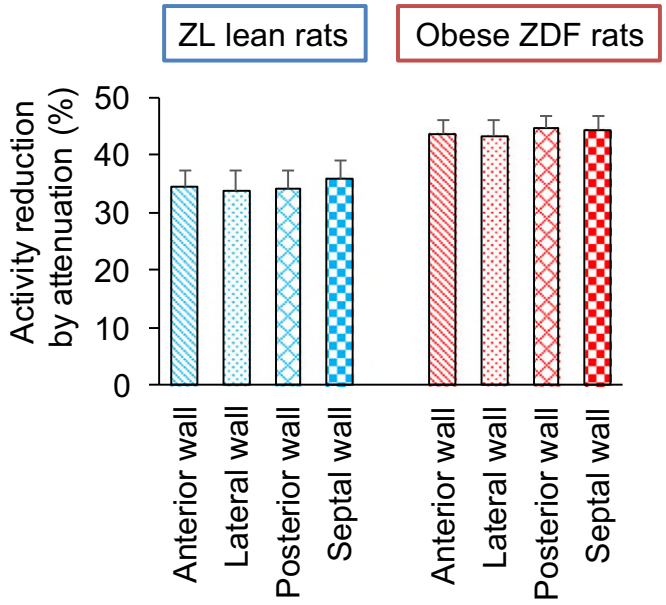

Fig. 3. Regional variation of attenuation among the four left ventricular walls in lean and obese rats. No significant differences are demonstrated between the walls in both Zucker lean (ZL lean rat) ($p = 0.73$) and Zucker diabetic fatty rats (obese ZDF rats) ($p = 0.65$).

5. Conclusion

Although tissue attenuation in cardiac PET images is much smaller in rodents than in human beings, its influence on quantification should not be ignored when small rodents with different body sizes are compared. In contrast, only a minimal impact of attenuation on the regional myocardial distribution pattern was demonstrated and might allow for

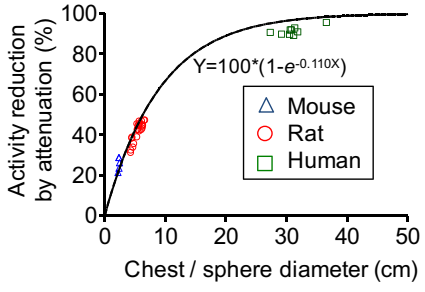

Fig. 4. Relationship between attenuation-caused myocardial activity reduction and chest diameter of mouse (triangle), rat (circle) and human (square). Solid line represents the theoretical curve of activity reduction by cylinder phantom computer simulation models with variable diameters, in which a point source is placed at the center. Linear attenuation coefficient of the phantom is that of acrylic (=0.110).

non-attenuation corrected assessment of myocardial tracer uptake defects.

.

Conflict of interest

The authors report no relationships that could represent a conflict of interest.

Acknowledgement of grant support

This work is partly supported by the Competence Network of Heart Failure funded by the Integrated Research and Treatment Center (IFB) of the Federal Ministry of Education and Research (BMBF 01EO1004) and the German Research Council (DFG grant HI 1789/2-1 and HI 1789/3-3).

References

[1] C. Anagnostopoulos, A. Georgakopoulos, N. Pianou, S.G. Nekolla, Assessment of myocardial perfusion and viability by Positron Emission Tomography, Int. J. Cardiol. 167 (2013) 1737–1749.

[2] F.M. Bengel, T. Higuchi, M.S. Javadi, R. Lautamäki, Cardiac positron emission tomography, J. Am. Coll. Cardiol. 54 (2009) 1–15.

[3] G.M. Boffa, P. Zanco, P. Della Valentina, P. Cardaioli, G. Thiene, R. Chioin, et al., Positron emission tomography is a useful tool in differentiating idiopathic from ischemic dilated cardiomyopathy, Int. J. Cardiol. 74 (2000) 67–74.

[4] M. Fiechter, C. Gebhard, J.R. Ghadri, T.A. Fuchs, A.P. Pazhenkottil, R.N. Nkoulou, et al., Myocardial perfusion imaging with 13N-Ammonia PET is a strong predictor for outcome, Int. J. Cardiol. 167 (2013) 1023–1026.

[5] T. Higuchi, C. Rischpler, K. Fukushima, T. Isoda, J. Xia, M.S. Javadi, et al., Targeting of endothelin receptors in the healthy and infarcted rat heart using the PET tracer 18F-FBzBMS, J. Nucl. Med. 54 (2013) 277–282.

[6] K. Toyoda, A. Nakano, Y. Fujibayashi, Y. Yonekura, T. Ueda, J.D. Lee, Diabetes mellitus impairs myocardial oxygen metabolism even in non-infarct-related areas in patients with acute myocardial infarction, Int. J. Cardiol. 115 (2007) 297–304.

[7] T. Higuchi, S.G. Nekolla, A. Jankaukas, A.W. Weber, M.C. Huisman, S. Reder, et al., Characterization of normal and infarcted rat myocardium using a combination of small-animal PET and clinical MRI, J. Nucl. Med. 48 (2007) 288–294.

[8] B. Bigalke, A. Phinikaridou, M.E. Andia, M.S. Cooper, A. Schuster, T. Wurster, et al., PET/CT and MR imaging biomarker of lipid-rich plaques using [64Cu]-labeled scavenger receptor (CD68-Fc), Int. J. Cardiol. 177 (2014) 287–291.

[9] A. Müller, L. Mu, R. Meletta, K. Beck, Z. Rancic, K. Drandarov, et al., Towards non-invasive imaging of vulnerable atherosclerotic plaques by targeting co-stimulatory molecules, Int. J. Cardiol. 174 (2014) 503–515.

[10] T. Higuchi, F.M. Bengel, Cardiovascular nuclear imaging: from perfusion to molecular function, Heart 94 (2008) 809–816.

[11] S.L. Bacharach, I. Buvat, Attenuation correction in cardiac positron emission tomography and single-photon emission computed tomography, J. Nucl. Cardiol. 2 (1995) 246–255.

[12] H. Zaidi, B. Hasegawa, Determination of the attenuation map in emission tomography, J. Nucl. Med. 44 (2003) 291–316.

[13] B. Nowak, M. Zimny, E.R. Schwarz, H.J. Kaiser, W. Schaefer, P. Reinartz, et al., Diagnosis of myocardial viability by dual-head coincidence gamma camera fluorine-18 fluorodeoxyglucose positron emission tomography with and without non-uniform attenuation correction, Eur. J. Nucl. Med. 27 (2000) 1501–1508.

[14] E.V. Garcia, Physical attributes, limitations, and future potential for PET and SPECT, J. Nucl. Cardiol. 19 (2012) 19–29.

[15] B.C. Millar, B.D. Prendergast, A. Alavi, J.E. Moore, 18FDG-positron emission tomography (PET) has a role to play in the diagnosis and therapy of infective endocarditis and cardiac device infection, Int. J. Cardiol. 167 (2013) 1724–1736.

[16] R. Yokoyama, M. Miyagawa, H. Okayama, T. Inoue, H. Miki, A. Ogimoto, et al., Quantitative analysis of myocardial 18 F-fluorodeoxyglucose uptake by PET/CT for detection of cardiac sarcoidosis ☆, Int. J. Cardiol. 195 (2015) 180–187.

[17] R.K. Chilukoti, A. Giese, W. Malenke, G. Homuth, A. Bukowska, A. Goette, et al., Atrial fibrillation and rapid acute pacing regulate adipocyte/adipositas-related gene expression in the atria, Int. J. Cardiol. 187 (2015) 604–613.

[18] Guide for the Care and Use of Laboratory Animals, eighth ed. National Academies Press (US), Washington (DC), 2011.

[19] J.G. Mannheim, M.S. Judenhofer, A. Schmid, J. Tillmanns, D. Stiller, V. Sossi, et al., Quantification accuracy and partial volume effect in dependence of the attenuation correction of a state-of-the-art small animal PET scanner, Phys. Med. Biol. 57 (2012) 3981–3993.

[20] Y.D. Son, H.K. Kim, S.T. Kim, N.B. Kim, Y.B. Kim, Z.H. Cho, Analysis of biased PET images caused by inaccurate attenuation coefficients, J. Nucl. Med. 51 (2010) 753–760.

[21] T.H. Marwick, R.T. Go, W.J. MacIntyre, G.B. Saha, D.A. Underwood, Myocardial perfusion imaging with positron emission tomography and single photon emission computed tomography: frequency and causes of disparate results, Eur. Heart J. 12 (1991) 1064–1069.

[22] B.J. Chow, S. Dorbala, M.F. Di Carli, M.E. Merhige, B.A. Williams, E. Veledar, J.K. Min, et al., Prognostic value of PET myocardial perfusion imaging in obese patients, JACC Cardiovasc. Imaging 7 (2014) 278–287.